Experimental Investigation and Numerical Treatment of Viscoelastic Materials

André Schmidt, Dr.-Ing and Lothar Gaul, Prof. Dr.-Ing. habil.
Institut für Angewandte und Experimentelle Mechanik, Universtät Stuttgart
Pfaffenwaldring 9, 70550 Stuttgart, Germany

Nomenclature

σ, ε	stress, strain
η	viscosity, loss factor
ν	Poisson's ratio
i	imaginary unit
E, E^*, E', E''	Young's modulus, complex Young's modulus, storage modulus, loss modulus
G, G^*, G', G''	shear modulus, complex shear modulus, storage modulus (shear), loss modulus (shear)
$E(t)$, $J(t)$	relaxation function, creep compliance
τ_{R}, τ_{C}	realxation time, retardation time
$_a\mathrm{D}_b^\alpha$	fractional derivative operator of order α with terminals a (lower) and b (upper)
Γ	Gamma function
Λ	logarithmic decrement
x, u	axis, displacement
ℓ, d, ρ	length, diameter, mass density
ω, f	angular frequency, frequency
c	speed of sound
F, T	force, temperature

ABSTRACT

Visoelastic material behavior is characterized by creep and relaxation processes for static loadings and damping in the case of dynamic harmonic loading. These phenomena are observed for all engineering materials to some extent. This paper gives an overview of classical linear viscoelastic material models and their limitations. The respective constitutive equations are first expressed as differential equations in time and are then generalized by the concept of fractional derivatives. This approach overcomes the disadvantages of classical models, leads to causal material behavior, and fulfills the second law of thermodynamics. As an example, experimental investigations conducted on an engineering plastic material yield its temperature und frequency dependent material properties. Based on the principle of thermorheologic simple material behavior, a so-called master curve is identified which maps the elastic and the dissipative properties of the material over an extensive frequency range. Finally, the material behavior is efficiently modeled with few material parameters through the use of fractional derivatives. The resulting constitutive equation is then used for further numerical calculations.

1 Introduction

The calculation of the dynamic behavior of any structure requires knowledge about its stiffness and its mass distribution. In addition, if energy dissipation cannot be neglected, the damping properties of the structure also have to be modeled. Measurements of the stiffness and the mass properties of engineering materials and their inclusion into any numerical calculation method such as the Finite Difference Method (FDM), the Finite Element Method (FEM), or the Boundary Element Method (BEM) does not present any serious difficulties. In contrast, the determination of a material's dissipative properties is a difficult task, especially if the amount of damping is low compared to the deformation energy of the structure under consideration. Moreover, the current techniques for modeling damping are in many cases insufficient.
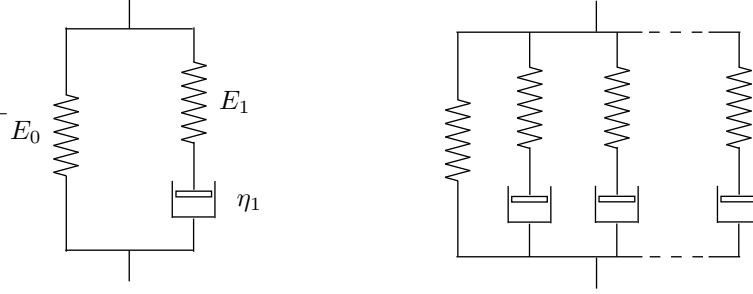
Figure 1: left: 3-parameter model; right: n-Parameter model

As long as a material or a complete structure is operated within its linear range or can be linearized about an operation point, linear viscoelastic models are used to describe the structure's damping properties [11]. One advantage of this approach is the possibility to carry out calculations both in the time domain and in the frequency domain. In addition, results from an (also linear) experimental modal analysis can directly be linked to numerical approaches. Linear viscoelastic constitutive equations can be written most generally in terms of hereditary integrals [4]. Alternatively, linear viscoelasticity can be defined by a differential equation relating the stresses and strains and their temporal derivatives.

Classical models of linear viscoelasticity predict a strong frequency dependence of the damping properties, whereas measurements on viscoelastic materials reveal a very small change in their dissipative behavior with varying frequency [11]. Thus, classical models have to be expanded to better concur with the measured data, which results in a high number of material parameters that have to be identified. Alternatively, the so-called model of constant hysteresis might be used in frequency-domain calculations. However, this model leads to non-causal material behavior in the time domain [8].

A better approximation is obtained by the use of fractional time derivatives [11]. These 'fractional models' have been verified to fulfill the second law of thermodynamics and show causal material behavior [13]. Thus, they can be used in time domain and in frequency domain calculations. The appearance of fractional derivatives in viscoelastic constitutive equations is physically sound [2, 6, 17, 21] and leads to models that concur well with the measured data over broad ranges of time or frequency with few material parameters [11]. This concept was first suggested by Gemant [10] in 1936 and had its revival by the research of Bagley and Torvik [1, 2] in the beginning of the 1980s.

2 Classical Models of Linear Viscoelasticity

Classical linear viscoelastic material models can be represented by an arbitrary composition of linear springs and dashpots. The simplest model for solids that is able to show all phenomena related to viscoelasticity is the 3-parameter model (also called 'standard linear solid' or 'Zener model'), see Fig. 1. Its constitutive equation is given by

$$\sigma + \frac{\eta_1}{E_1}\dot{\sigma} = E_0\varepsilon + \eta_1\frac{E_0 + E_1}{E_1}\dot{\varepsilon}. \tag{1}$$

Regarding the definition of viscoelasticity by means of hereditary integrals, the relaxation function $E(t)$ and the creep compliance $J(t)$ (the material's answer to a single step in load) can be derived from Eq. (1), see [20]

$$E(t) = E_0 + E_1 e^{-t/\tau_{\mathrm{R}}}, \quad t > 0, \qquad J(t) = \frac{1}{E_0} - \frac{E_1}{E_0(E_0 + E_1)}e^{-t/\tau_{\mathrm{C}}}, \quad t > 0 \tag{2}$$

where $\tau_{\mathrm{R}} = \eta_1/E_1$ denotes the relaxation time and $\tau_{\mathrm{C}} = \eta_1(E_0 + E_1)/(E_0 E_1)$ is called the retardation time. Using the principle of superposition, the answer of the model to an arbitrary load can be found as [20]

$$\sigma(t) = \varepsilon(t)E(0) + \int_0^t \varepsilon(\tau)\dot{E}(t - \tau)\,\mathrm{d}\tau \qquad \text{or} \qquad \varepsilon(t) = \sigma(t)J(0) + \int_0^t \sigma(\tau)\dot{J}(t - \tau)\,\mathrm{d}\tau. \tag{3}$$
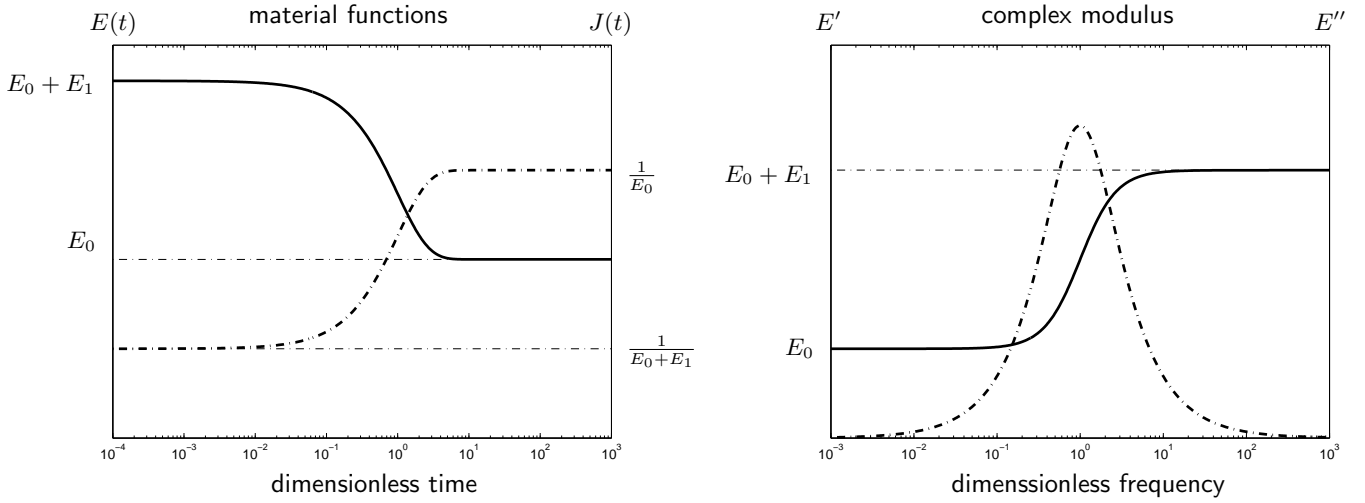
Figure 2: Characteristics of the 3-parameter model — left: stress relaxation (solid), creep function (dashed); right: storage modulus (solid), loss modulus (dashed)

Transferring Eq. (1) into the frequency domain yields

$$\tilde{\sigma} = \frac{E_0 + \mathrm{i}\,\eta_1\omega\,\frac{E_0+E_1}{E_1}}{1 + \mathrm{i}\,\frac{\eta_1\omega}{E_1}}\,\tilde{\varepsilon} = E^*\tilde{\varepsilon}\,, \qquad\qquad E^* = E' + \mathrm{i}E'' = (1+\mathrm{i}\eta)E' \qquad (4)$$

where a tilde denotes the Fourier transformed and E^* is called the complex modulus. The latter consists of the storage modulus E' and the loss modulus E'' and can alternatively be written in terms of the loss factor η. For the 3-parameter model one obtains

$$E' = \frac{E_0 + (\eta_1\omega)^2\,\frac{E_0+E_1}{E_1^2}}{1 + \left(\frac{\eta_1\omega}{E_1}\right)^2}\,, \qquad\qquad E'' = \frac{\omega\eta_1}{1 + \left(\frac{\eta_1\omega}{E_1}\right)^2}\,. \qquad (5)$$

The time- and the frequency-dependent properties of the 3-parameter model are displayed in Fig. 2 on half-logarithmic scales. By adjusting the free parameters one can control the respective magnitudes and relaxation or retardation times of the curves. But all curves will only be 'active' within approximately two decades in time or frequency. Since most materials show a weak frequency dependence over many decades, classical viscoelastic models are extended by a number of spring/dashpot combinations as displayed in Fig. 1. The resulting constitutive equations can be written in the form

$$\sum_{k=0}^{n} p_k \mathrm{D}^k \sigma = \sum_{k=0}^{m} q_k \mathrm{D}^k \varepsilon\,, \qquad (6)$$

where the operator D^k denotes the derivative of order k with respect to time and p_k, q_k are material-dependent coefficients. In viscoelastic models according to Fig. 1 the number $m = n$ equals the number of Maxwell elements (spring-dashpot combinations connected in series). The relaxation function and the creep function are deduced by means of a Laplace transformation [20] and can be written in the form

$$E(t) = E_0 + \sum_{i=1}^{n} E_i \mathrm{e}^{-t/\tau_{R_i}}\,, \qquad\qquad J(t) = J_0 + \sum_{i=1}^{n} J_i \mathrm{e}^{-t/\tau_{C_i}}\,, \qquad (7)$$

where τ_{C_i} and τ_{R_i} are the different creep and relaxation times, respectively. The frequency-domain representation of Eq. (6) results in

$$\tilde{\sigma} = \frac{\sum_{k=0}^{m} q_k (\mathrm{i}\omega)^k}{\sum_{k=0}^{n} p_k (\mathrm{i}\omega)^k}\,\tilde{\varepsilon} = E^*\tilde{\varepsilon}\,. \qquad (8)$$

The respective time- and frequency-dependent constitutive behavior is depicted in Fig. 3. The resulting curves can be interpreted as a superposition of n curves as they are obtained from the 3-parameter model, see Fig. 2. Thus, the curves still show a strong frequency dependency that now covers a broader range of time and frequency at the expense of an increasing number of material parameters. In practice, commonly one Maxwell element is added for each decade in time or frequency as a compromise between the objectionable overshooting behavior and the number of material parameters.
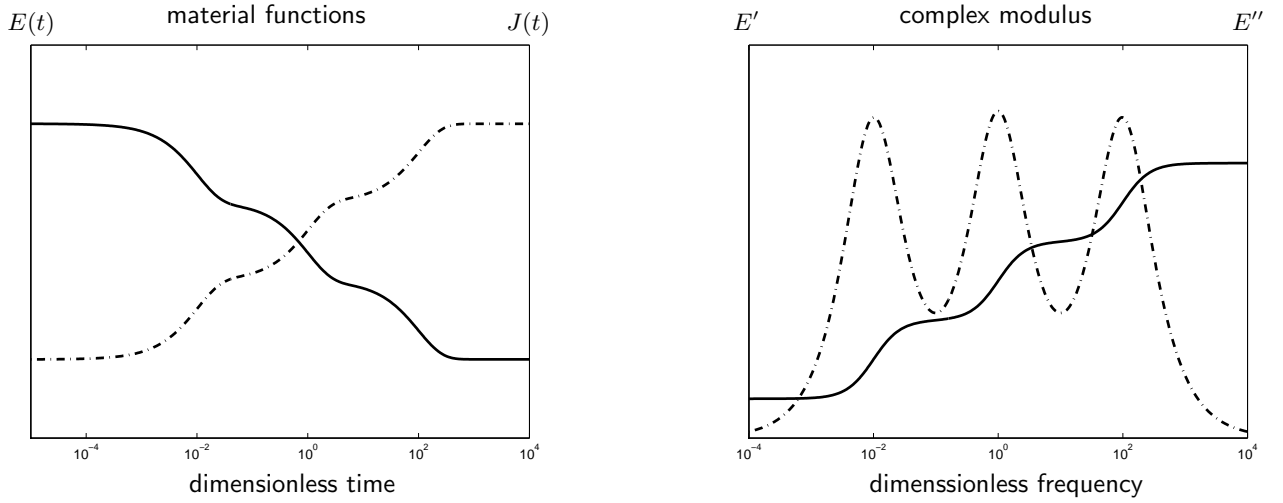
Figure 3: Characteristics of an n-parameter model (for $n = 7$) — left: stress relaxation (solid), creep function (dashed); right: storage modulus (solid), loss modulus (dashed)

3   Fractional Models of Linear Viscoelasticity

A generalization of classical viscoelastic models is obtained by the use of fractional derivatives instead of integer-order derivatives. A fractional derivative of order α of a function $f(t)$ with respect to time is given by (Riemann-Liouville definition, see e.g. [14, 16])

$$_a\mathrm{D}_t^\alpha f(t) = \mathrm{D}^n \left[_a\mathrm{D}_t^{\alpha-n} f(t) \right] = \frac{1}{\Gamma(n-\alpha)} \mathrm{D}^n \left[\int_a^t \frac{f(\tau)}{(t-\tau)^{\alpha+1-n}} \, \mathrm{d}\tau \right], \qquad n \in \mathbb{N}, \, \alpha \in \mathbb{R}, \, n > \alpha, \tag{9}$$

where $\Gamma(x) = \int_0^\infty y^{x-1} \mathrm{e}^{-y} \, \mathrm{d}y$ is the Gamma function. Eq. (9) provides the classical derivatives for $\alpha \in \mathbb{N}$. Note that in contrast to integer-order derivatives a fractional derivative is a non-local operator since the history of the function in the interval $[a, t]$ contributes to its actual value, similar to an integration. The question of what value has to be taken for the lower boundary a depends on the physical interpretation of the underlying problem. In general, the lower boundary (also called 'terminal') is set to $a = -\infty$. The Fourier transformation of a fractional derivative of a function $f(t)$ leads to

$$\mathcal{F} \left[_{-\infty}\mathrm{D}_t^\alpha f(t) \right] = (\mathrm{i}\omega)^\alpha \tilde{f}, \tag{10}$$

where $\tilde{f}$ is the Fourier transformed of the function f.

So-called 'fractional constitutive equations' can be derived by simply replacing the integer-order derivatives in Eq. (6) by fractional derivatives [7]. In this case, additional conditions have to be fulfilled to ensure the constitutive behavior of a solid and purely dissipative behavior [13]. An alternative way that overcomes this difficulty makes use of a generalized damping element that is also called a 'fractional element' or a 'spring-pot' [12], see Fig. 4

$$\sigma = p_{-\infty}\mathrm{D}_t^\alpha \varepsilon, \tag{11}$$

that obtains the order of derivative α as an additional free parameter. The constitutive behavior of a spring and a dashpot are obtained for $\alpha = 0$ and $\alpha = 1$, respectively. The capabilities of a solid are assured by simply replacing the dash-pots of a respective classical model by fractional elements. In case of the classical 3-parameter model one arrives at the 'fractional 3-parameter model' and its constitutive equation

$$\sigma + \frac{p}{E_1} {}_{-\infty}\mathrm{D}_t^\alpha \sigma = E_0\varepsilon + p \frac{E_0 + E_1}{E_1} {}_{-\infty}\mathrm{D}_t^\alpha \varepsilon. \tag{12}$$

Using relation (10), the constitutive equation (12) can be transformed into the frequency domain

$$\tilde{\sigma} = \frac{E_0 + (\mathrm{i}\omega)^\alpha p \frac{E_0 + E_1}{E_1}}{1 + (\mathrm{i}\omega)^\alpha \frac{p}{E_1}} \tilde{\varepsilon} = E^* \tilde{\varepsilon}. \tag{13}$$
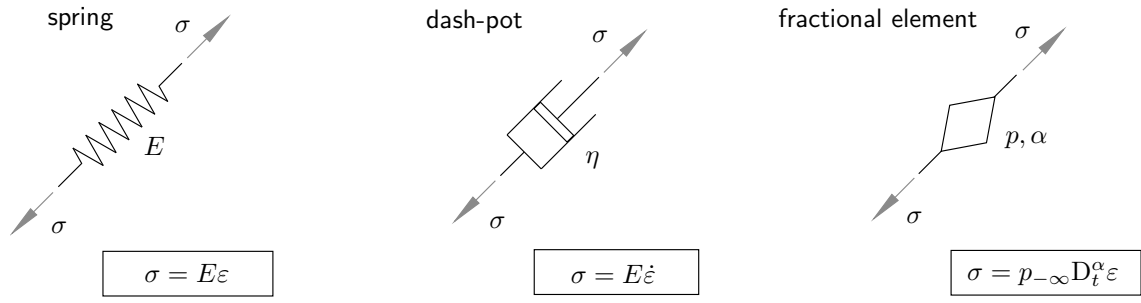
Figure 4: Illustration of the generalized 'fractional' element

From Eqns. (10) and (13) it becomes obvious that the frequency dependence of the model's properties is directly linked to the order of derivative α and becomes weaker for decreasing α.

Regarding the hereditary integral formulation, the relaxation function $E(t)$ or the creep compliance $J(t)$ can be calculated from (12), see [3]

$$E(t) = E_0 + E_1\,\mathcal{E}_\alpha\left(-\frac{E_1}{p}t^\alpha\right) \qquad J(t) = \frac{1}{E_0} - \frac{E_1}{E_0(E_0+E_1)}\,\mathcal{E}_\alpha\left(-\frac{E_0 E_1}{p(E_0+E_1)}t^\alpha\right) \tag{14}$$

where

$$\mathcal{E}_\alpha(x) = \sum_{k=0}^{\infty} \frac{x^k}{\Gamma(\alpha k + 1)} \tag{15}$$

is the Mittag-Leffler function which can be interpreted as a generalized exponential function. The influence of the order of derivative α on the material functions is depicted in Fig. 5. Similar to the frequency dependence, the time dependence is reduced with decreasing α and leads to a smoother changeover from the initial values to the long-term properties.

4 Experimental investigations

As an example, the engineering plastic Delrin$^{\text{TM}}$ 100 manufactured by DuPont company is considered. Delrin$^{\text{TM}}$ is a thermoplastic polyoxymethylene (POM) that is widely used in technical applications (e.g. as zippers or gears) due to its relatively high stiffness combined with a low friction coefficient.

The experiments are performed by a testing machine RMS-800/RDSII (Rheometrics) in which a sample is subjected to sinusoidal rotational deformations and the resulting torque is measured. Since the sample's dimensions are known, the shear stress $\tau = \hat{\tau}\sin(\omega t)$ and the shear strain $\varepsilon = \hat{\varepsilon}\sin(\omega t - \Phi_0)$ can easily be determined. The complex shear modulus $G^* = G' + iG''$ then is calculated from the stress amplitude $\hat{\tau}$, the strain amplitude $\hat{\varepsilon}$, and the phase angle Φ_0

$$G' = \frac{\hat{\varepsilon}}{\hat{\tau}} \qquad\qquad G'' = \tan\Phi_0\,G'. \tag{16}$$

The measurements are accomplished within a temperature range from -20°C up to 50°C in steps of 2°C each of which including the frequencies 1 Hz, 2 Hz, 5 Hz, 10 Hz, 20 Hz and 50 Hz.

Assuming thermo-rheological simple material behavior, a so-called master curve is constructed for a reference temperature $T_0 = 0^\circ$C. For this purpose, a function γ is identified that 'shifts' the measured complex modulus $G^*(f_2, T_2)$ at a distinct frequency f_2 and temperature T_2 to some 'reduced frequency' f_1 at the reference temperature T_0 [11]

$$G^*(f_1, T_0) = G^*(f_2\gamma(T_2, T_0), T_0). \tag{17}$$

Although some analytical functions $\gamma(T, T_0)$ are suggested in the literature (WLF equation, Arrhenius equation), the best result is found from individually defining the shift factor $\gamma_i(T_i, T_0)$ at each temperature T_i of the measurements. This can easily be done since the measured data exhibits some overlapping area, see Fig. 6.
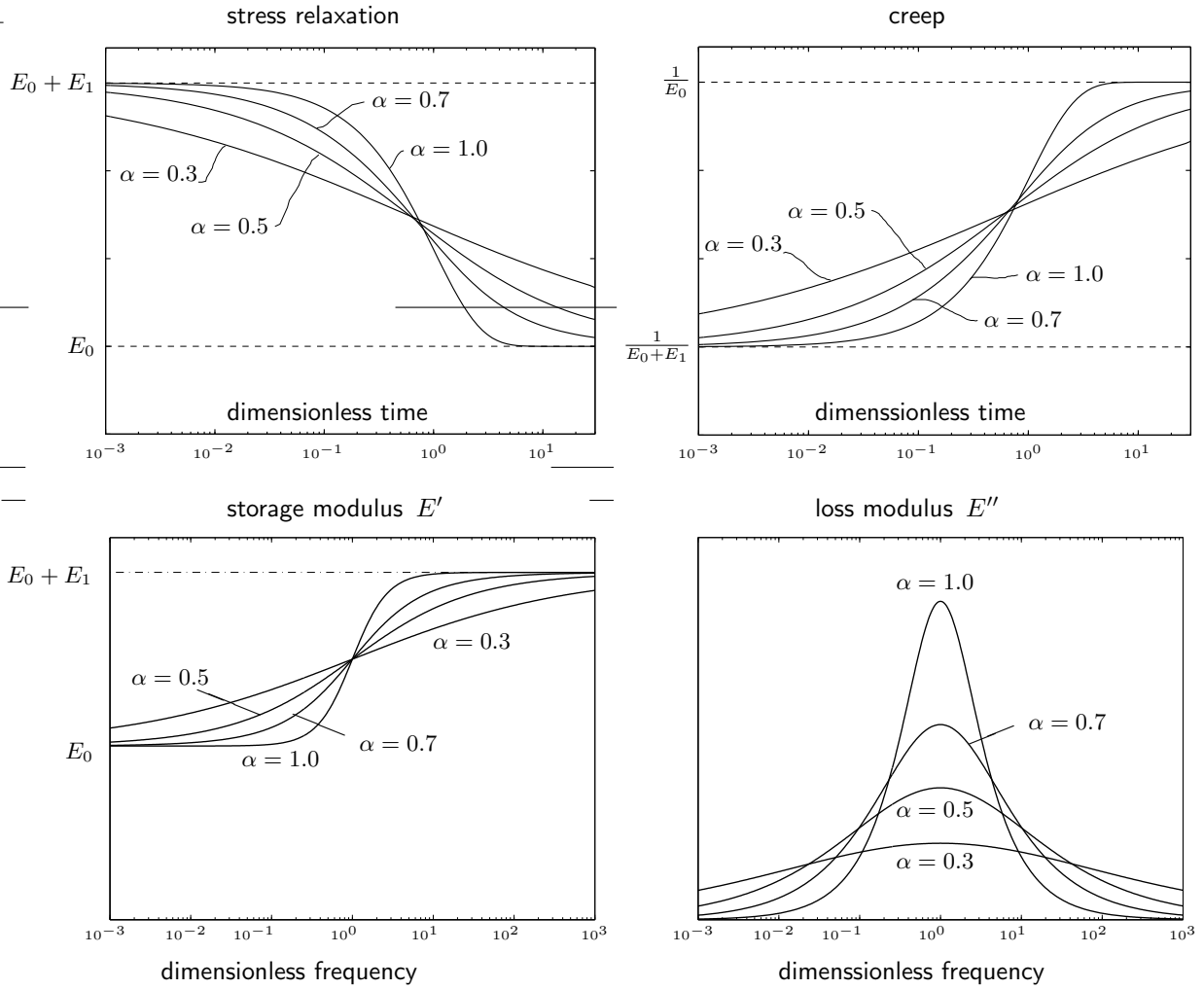
Figure 5: Time- and frequency-dependent behavior of the n-parameter model (for n=7)

5 Parameter identification

The complex modulus given by the master curve covers a range of approximately 30 decades in frequency. Following the 'rule' from practical experience with classical models, a model consisting of 30 Maxwell elements (i.e. 61 free parameters) has to be identified. This is done by means of a least-squares fit where the residuum R to be minimized is given by

$$R = \sum_{i=1}^{i_{\max}} \left[(G'_{i,\text{measured}} - G'_{i,\text{model}})^2 + a^2 (G''_{i,\text{measured}} - G''_{i,\text{model}})^2 \right] . \tag{18}$$

For the identification all available data points are used. The residuum of the imaginary parts is weighted by a factor of a^2 where

$$a = \frac{G'_{\max,\text{measured}}}{G''_{\max,\text{measured}}} \tag{19}$$

is the proportion of the highest measured storage and loss modulus, respectively. The result displayed in Fig. 6 shows an extensive overshooting behavior associated with poor extrapolation properties.

In contrast, a fractional model depicted in Fig. 7 is identified using the same method Eq. (18). The model consists of 7 free parameters including the orders of derivatives α_1 and α_2. The identified parameters are given in Table 1. In comparison to the classical approach, the residuum is reduced by 42.4% whereas the fractional model requires only few parameters, does not show any overshooting behavior, and holds reasonable extrapolation properties, see Fig. 6. By a change of the
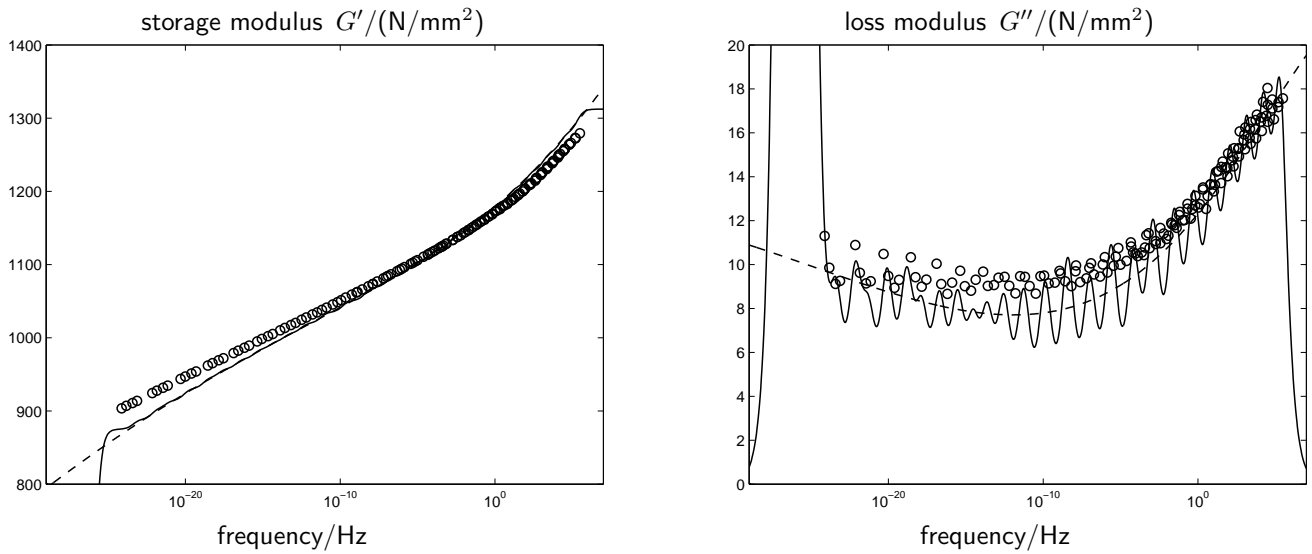
Figure 6: Master curve for Delrin^TM at $0°C$ obtained from shifted measured data (o) and parameter identifications with a classical 61-parameter model (solid) and a fractional 5-parameter model (dashed)

weighting factor w, an improved fit to the storage modulus can be achieved at the expense of a reduced fit to the loss modulus.

Table 1: Identified material parameters for shear deformation

$G_0/\frac{N}{mm^2}$	$G_1/\frac{N}{mm^2}$	$p_1/\frac{Ns^{\alpha_1}}{mm^2}$	α_1	$G_2/\frac{N}{mm^2}$	$p_2/\frac{Ns^{\alpha_2}}{mm^2}$	α_2
0.0	514.4	77.2	0.0794	1 324.2	7 198.5	0.0202

6 Example

The concept of fractional derivatives in linear viscoelasticity can directly be implemented into the Finite Difference Method (FDM) [19], the Boundary Element Method (BEM) [7, 9], and the Finite Element Method (FEM) [5, 15, 18] in the time domain and in the frequency domain. As an example, the dynamic response of a viscoelastic rod made of Delrin^TM is calculated. For this purpose, the identified fractional viscoelastic model is converted from shear deformation to axial deformation using the relationship $E^* = 2G^*(1+\nu)$, where a Poisson's ratio $\nu = 0.39$ is used (Table 2). The rod is fixed at $x = 0$ and subjected to a single step in load $F(t) = 100\,N\,h(t)$ at its free end $x = \ell$. The time-domain calculation is performed with the FDM where the discretization in time (Central Difference Method) and in space is of second-order accuracy, see [19]. The rod and its discretization are depicted in Fig. 8 where the total number of spatial nodes is $n = 30$.
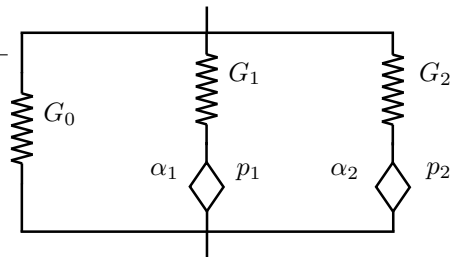
Figure 7: Fractional 5-parameter model

Table 2: Converted material parameters for axial deformation

$E_0/\frac{\text{N}}{\text{mm}^2}$	$E_1/\frac{\text{N}}{\text{mm}^2}$	$p_1/\frac{\text{Ns}^{\alpha_1}}{\text{mm}^2}$	α_1	$E_2/\frac{\text{N}}{\text{mm}^2}$	$p_2/\frac{\text{Ns}^{\alpha_2}}{\text{mm}^2}$	α_2
0.0	1 430.1	214.6	0.0794	3 681.3	20 011.8	0.0202
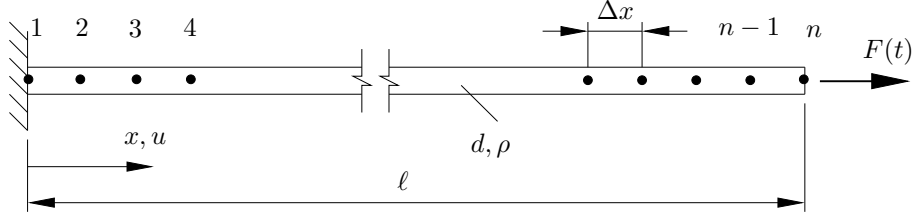
Figure 8: FDM discretization of the rod together with its boundary conditions

Since the length of the rod is $\ell = 2\,\text{m}$, the nodal distance is given by $\Delta x \approx 69\,\text{mm}$. The cross section of the rod is circular (diameter $d = 15\,\text{mm}$) and the density of Delrin$^{\text{TM}}$ is $\rho = 1\,420\,\frac{\text{kg}}{\text{m}^3}$. The whole simulation time is $0.6\,\text{s}$ were a time step size $\Delta t = 40\mu\text{s}$ is used, resulting in $15\,000$ time steps.

The calculated deflection of the rod's free end is displayed in Fig. 9. Since the force $F(t)$ is acting during the whole simulation time, the decaying oscillation is superimposed by a creep process. The neutral position u_{np} can be calculated from the oscillating displacement signal using three successive extrema $u_{\text{ex},1}$, $u_{\text{ex},2}$, and $u_{\text{ex},3}$

$$u_{\text{np}} = \frac{u_{\text{ex},1}u_{\text{ex},3} - u_{\text{ex},2}^2}{u_{\text{ex},1} - 2u_{\text{ex},2} + u_{\text{ex},3}}. \tag{20}$$

The creep process detected from the calculated oscillation is also shown in Fig. 9.

A verification of the parameter identification and the implementation of the fractional constitutive equation into the FDM scheme can be achieved by detecting the complex modulus from the simulation's results. The first eigenfrequency f of a rod that is fixed at one end is given by

$$f = \frac{c}{4\ell}, \tag{21}$$

where $c = \sqrt{E/\rho}$ is the speed of sound. The frequency $f = 194.1\,\text{Hz}$ is identified from the calculated oscillation. Since the storage modulus for low-loss materials is in very good approximation equal to Young's modulus E one obtains

$$E' \approx E = 16\rho\ell^2 f^2 = 3\,423.4\,\frac{\text{N}}{\text{m}^2}. \tag{22}$$

The loss modulus is detected from the logarithmic decrement

$$\Lambda = \frac{1}{k}\ln\frac{\hat{x}_n}{\hat{x}_{n+k}} = 0.03970, \tag{23}$$

where the amplitudes $\hat{x}_n$ and $\hat{x}_{n+k}$ are the maxima after $n = 15$ and $n + k = 115$ oscillations with respect to the tip's neutral position. Thus, the first 14 oscillations are skipped to let the transients die out. This finally leads to

$$E'' \approx \frac{\Lambda}{\pi}E' = 43.26\,\frac{\text{N}}{\text{m}^2}. \tag{24}$$

In order to compare the results with the data from the experiments the respective shear moduli

$$G' = \frac{E'}{2(1+\nu)} = 1\,231.4\,\frac{\text{N}}{\text{m}^2} \qquad\qquad G'' = \frac{E''}{2(1+\nu)} = 15.56\,\frac{\text{N}}{\text{m}^2} \tag{25}$$

are calculated. As depicted in Fig. 10 the results are in very good agreement with the measured data. Thus, the parameter identification and the numerical implementation are proven to be correct.
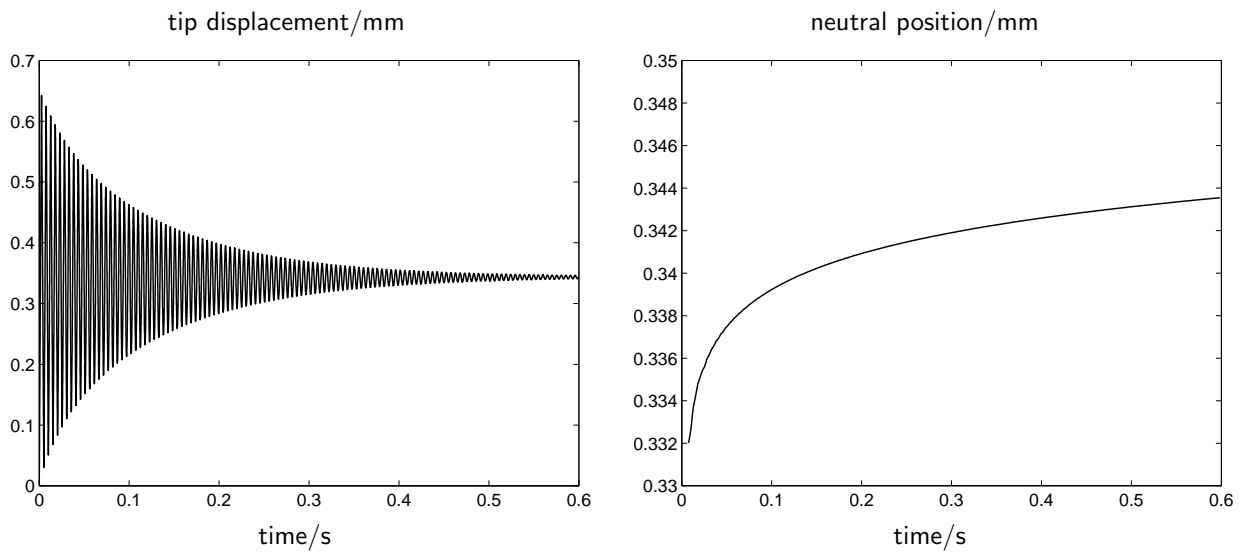
Figure 9: Decaying free oscillation of the rod's tip (left) and its neutral position (right)

7   Summary

Linear viscoelastic constitutive equations are usually modeled by means of spring-dashpot combinations. Such models result in integer-order differential equations and exponential functions as kernels in hereditary integral formulations for solid materials. This approach shows substantial deficiencies when measured material behavior has to be modeled over broad ranges of time or frequency. An alternative approach makes use of fractional derivatives where the order of derivative is interpreted as a free parameter that can become any real number. The curve-fitting properties of such models improve significantly while causal material behavior and thermo-mechanical consistency is assured. The models need only few parameters and can be implemented into numerical methods for structural calculations. As an example, an engineering plastic was investigated experimentally, and a master curve was deduced on the basis of thermo-rheologically simple material behavior. A classical and a fractional-derivative model were identified in order to highlight the advantages of the new approach. Finally, a numerical calculation of the dynamic response of a plastic rod was accomplished with the Finite Difference Method in the time domain. The results of the calculation were used to confirm the parameter identification and the numerical implementation of the fractional-derivative model.
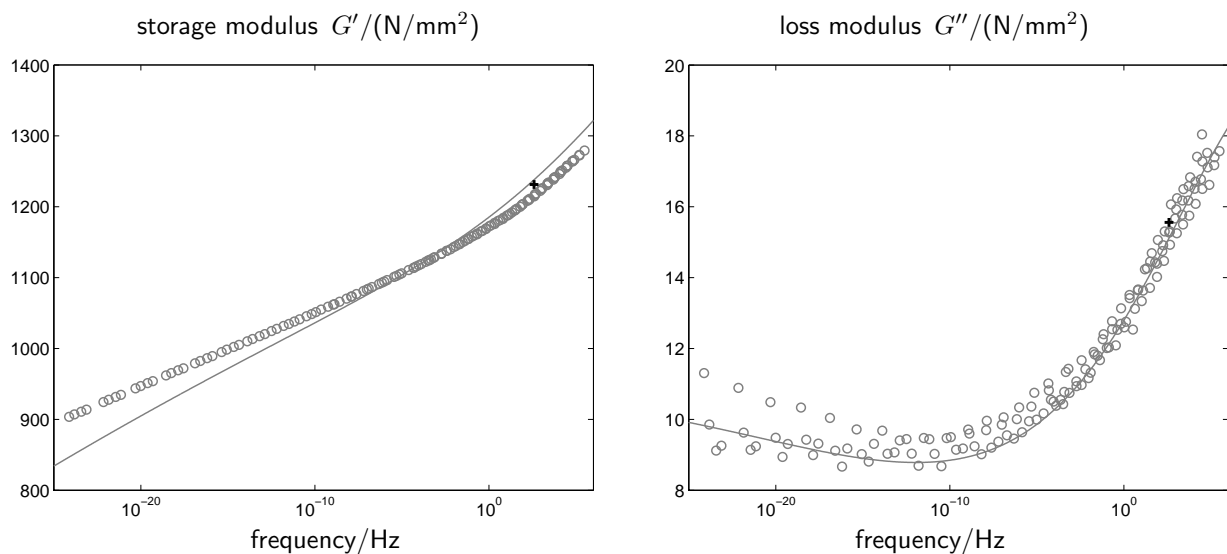
Figure 10: Complex modulus: measured data (o), fractional 5-parameter model (—), FDM calculation (+)

References

[1] BAGLEY, R. L., AND TORVIK, P. J. Fractional calculus — a different approach to the analysis of viscoelastically damped structures. *AIAA Journal 21*, 5 (1983), 741–748.

[2] BAGLEY, R. L., AND TORVIK, P. J. A theoretical basis for the application of fractional calculus to viscoelasticity. *Journal of Rheology 27*, 3 (1983), 201–210.

[3] CAPUTO, M., AND MAINARDI, F. Linear models of dissipation in anelastic solids. *Rivista del Nuovo Cimento 1*, 2 (1971), 161–198.

[4] CHRISTENSEN, R. M. *Theory of Viscoelasticity*. Academic Press, New York, 1971.

[5] ENELUND, M., AND JOSEFSON, L. Time-domain finite element analysis of viscoelastic structures with fractional derivatives constitutive relations. *AIAA Journal 35*, 10 (1997), 1630–1637.

[6] FERRY, J. D., LANDEL, R. F., AND WILLIAMS, M. L. Extensions to the rouse theory of viscoelastic properties to undiluted linear polymers. *Journal of Applied Physics 26*, 4 (1955), 359–362.

[7] GAUL, L. The influence of damping on waves and vibrations. *Mechanical Systems and Signal Processing 13*, 1 (1999), 1–30.

[8] GAUL, L., BOHLEN, S., AND KEMPFLE, S. Transient and forced oscillations of systems with constant hysteretic damping. *Mechanics Research Communications 12*, 4 (1985), 187–201.

[9] GAUL, L., AND SCHANZ, M. Dynamics of viscoelastic solids treated by boundary element approaches in time domain. *European Journal of Mechanics, A/Solids 13*, 4 (1994), 43–59.

[10] GEMANT, A. A method of analyzing experimental results obtained from elasto-viscous bodies. *Physics 7* (1936), 311–317.

[11] JONES, D. I. *Viscoelastic Vibration Damping*. John Wiley & Sons, New York, 2001.

[12] KOELLER, R. C. Application of fractional calculus to the theory of viscoelasticity. *Journal of Applied Mechanics 51* (1984), 299–307.

[13] LION, A. On the thermodynamics of fractional damping elements. *Continuum Mechanics and Thermodynamics 9*, 2 (1997), 83–96.

[14] OLDHAM, K. B., AND SPANIER, J. *The Fractional Calculus*. Academic Press, New York and London, 1974.

[15] PADOVAN, J. Computational algorithms for fe formulations involving fractional operators. *Computational Mechanics 2* (1987), 271–287.

[16] PODLUBNY, I. *Fractional Differential Equations*. Academic Press, San Diego and London, 1999.

[17] ROUSE, P. E. J. The theory of linear viscoelastic properties of dilute solutions of coiling polymers. *The Journal of Chemical Physics 21*, 7 (1953), 1272–1280.

[18] SCHMIDT, A., AND GAUL, L. Finite element formulation of viscoelastic constitutive equations using fractional time derivatives. *Journal of Nonlinear Dynamics 29* (2002), 37–55.

[19] SCHMIDT, A., AND GAUL, L. On the numerical evaluation of fractional derivatives in multi-degree-of-freedom systems. *Signal Processing 86*, 10 (2006), 2592–2601.

[20] WINEMAN, A. S., AND RAJAGOPAL, K. R. *Mechanical Response of Polymers*. Cambridge University Press, Cambridge, 2000.

[21] ZIMM, B. H. Dynamics of polymer molecules in dilute solution: viscoelasticity, flow birefringence and dielectric loss. *The Journal of Chemical Physics 24*, 2 (1956), 269–278.